MEDEA

Multidimensional seismic risk assessment through explainable artificial intelligence

Deliverable 3.2.: New classes of structures and new benchmark structures

MULTIDIMENSIONAL SEISMIC RISK ASSESSMENT COMBINING STRUCTURAL DAMAGES AND PSYCHOLOGICAL CONSEQUENCES USING EXPLAINABLE ARTIFICIAL INTELLIGENCE

Co-funded by the European Union

Deliverable Title	**New classes of structures and new benchmark structures**
Deliverable number	**3.2**
Deliverable Lead:	eCampus
Related Work Package:	WP3: Benchmark structures, EDPs, and representative families
Author(s):	Fabrizio Comodini, Elisabetta Cattoni, Salvatore Verre, Riccardo Panico (eCampus)
Dissemination Level:	Public
Due Submission Date:	30/05/24
Actual Submission:	17/06/24
Project Number	101101236
Status	Version 1.0 (17/06/24)
Reviewed (Authors)	Fabrizio Comodini, Elisabetta Cattoni, Salvatore Verre, Riccardo Panico (eCampus)
Start Date of Project:	01/12/22
Duration:	24 months
Abstract	This deliverable provides criteria used to define new classes of structures and the new benchmark structures in an existing class. For each new class, the criteria to define technical parameters are presented along with their dependency on geometric and mechanical properties of the structure. For buildings with reinforced concrete and masonry structure and for retaining walls, the procedures used to determine the engineering demand parameters (EDPs) and peak ground accelerations associated with predefined levels of damage (capacity PGAs) are described. These procedures have to be used when adding new benchmarks for improving the accuracy of the results in terms of capacity PGAs.
Status changes history	Version 1.0 (16/06/24) – First release

Co-funded by the European Union

Funded by the European Union. Views and opinions expressed are however those of the author(s) only and do not necessarily reflect those of the European Union. Neither the European Union nor the granting authority can be held responsible for them.

TABLE OF CONTENTS

Co-funded by the European Union

Funded by the European Union. Views and opinions expressed are however those of the author(s) only and do not necessarily reflect those of the European Union. Neither the European Union nor the granting authority can be held responsible for them.

ABBREVIATIONS

MEDEA	**Multidimensional Seismic Risk Assessment Combining Structural Damages And Psychological Consequences Using Explainable Artificial Intelligence**
EDP	Engineering Demand Parameter
PGA	Peak Ground Acceleration
TP	Technical parameter
XAI	eXplainable Artificial Intelligence
FE	Finite element

Co-funded by the European Union

Funded by the European Union. Views and opinions expressed are however those of the author(s) only and do not necessarily reflect those of the European Union. Neither the European Union nor the granting authority can be held responsible for them.

1. INTRODUCTION

The overarching goal of the MEDEA project is to enhance cross-border disaster risk management by focusing on prevention and preparedness in Europe and neighboring EU countries. Specifically, the project aims to mitigate the impact of seismic events and enhance resilience, defined as the capacity to withstand, absorb, adapt to, and recover from earthquakes efficiently and promptly. To achieve this objective, the project proposes developing an intelligent system for multidimensional seismic risk assessment in cross-border regions. Using artificial intelligence, this system aims to estimate earthquake-induced losses by predicting structural damage, such as building collapses, while also forecasting the psychological ramifications for affected individuals. Integrating psychological consequences, the project will investigate familial and individual factors and relational and contextual aspects that may exacerbate psychological distress among family members in the aftermath of seismic events. By assessing potential medium and long-term psychological effects on those involved in earthquakes, the project seeks to identify high-risk families susceptible to psychological distress, thereby anticipating and preventing the onset of post-traumatic stress disorder (PTSD).

Within the framework of the MEDEA project, the specific objectives Work Package 3 "*Benchmark structures, EDPs, and representative families*" are: i) Identification of benchmark structures; ii) Selection and calculation of the best EDPs to quantify the effect of seismic actions on structures; iii) Identification of the representative families. This deliverable focuses on the definition of classes of structures having similar characteristics in terms of materials and geometry, the definition of the EDPs used to quantify the effects of seismic actions, and the criteria used to define benchmark structures and to determine the values of their EDPs.

This deliverable is organized as follows: Section 2 presents the criteria used to define new classes of structures. Section 3 defines a metric among structures used to establish whenever further benchmark structures have to be added and provides the procedure to evaluate their EDPs and capacity PGAs. Finally, Section 4 presents the conclusion.

Co-funded by the European Union

Funded by the European Union. Views and opinions expressed are however those of the author(s) only and do not necessarily reflect those of the European Union. Neither the European Union nor the granting authority can be held responsible for them.

2. DEFINITION OF NEW CLASSES OF STRUCTURES

Within the project, each structure is identified by a set of technical parameters (TPs) that are used in the eXplainable Artificial Intellicence (XAI) algorithm to determine the seismic capacity of a given structure. In particular, XAI uses TPs to assess similarity between a given real structure and the structures belonging to a certain class. Then, engineering demand parameters (EDPs) and seismic capacity of the real structure is evaluated based on the capacity of the benchmark structures belonging to the class. This procedure requires that structures are divided in classes based on their TPs. Each class is identified by a specific set of TPs. When it is necessary to evaluate the seismic capacity of a structure that can't be represented by the TPs of the classes previously defined, it is necessary to define a new class. For example, retaining walls can't be defined by the same TPs used for masonry and reinforced concrete building structures, therefore a class of retaining wall structures had to be defined in order to determine their seismic capacity. The definition of a new class requires the following steps:

- Identification of the typology of structures to be included in the class. The typology of the structures to be included in the class has to be accurately defined in terms of type of structural elements, geometrical properties, typical structural response and failure mechanisms.
- Identification of the structural data that describe the geometrical and mechanical properties of the structures of the class.
- Identification of the representative TPs. Based on the structural data a number of TPs is derived. While the number of structural data can be different for different structures belonging to a certain class (e.g., the number of TPs of reinforced concrete structures is different from that of masonry structures and retaining walls), the number of TPs has to be the same for all the structures belonging to the class (e.g., for multistorey buildings, global TPs have to be properly defined, since the number of TPs cannot depend on the number of storeys or on the structure geometry). The choice of the TPs is not unique: different sets of TPs have to be processed in order to determine (via XAI, as described in Deliverable 4.1) the set providing the best results in terms of correlation between TPs and EDPs and seismic capacity. Typical TPs are the seismic masses, average stresses produced by gravity loads, stiffnesses, natural period, and material and soil characteristics.

Co-funded by the European Union

Funded by the European Union. Views and opinions expressed are however those of the author(s) only and do not necessarily reflect those of the European Union. Neither the European Union nor the granting authority can be held responsible for them.

- Identification of the engineering demand parameters (EDPs) that measure the effect of a seismic action on the structures of the class and the criteria to obtain the seismic capacity based on the EDPs. The choice of the EDPs is strongly related to the type of structural elements (e.g., EDPs characterizing the reinforced concrete columns are different than those characterizing the reinforced concrete beams, masonry panels, etc.).
- Construction of a dataset of benchmark structures that represent the characteristics of the structures belonging to the class. Each benchmark structure is identified by a specific set of values of TPs. In order to obtain a complete representation of the structures of the class, a range of typical values of each TP have to be established. Each benchmark structure is then identified by a combination of values of TPs within their specific ranges. A wide number of significant combinations of TPs has to be defined in order to represent properly the different configurations of the structures in the class.
- Structural analysis of benchmark structures with the aim of obtaining their EDPs and capacity PGAs. The type of analysis to be performed depends on the characteristics of the structures. For all type of structure, the capacity PGAs, including the values corresponding to the damage control and collapse prevention damage states (life-saving limit state and collapse limit state) have to be computed. In these conditions, the structure experiences large inelastic deformations, therefore nonlinear structural analysis is recommended.

Finally, the dataset of benchmark structures of the class will include the values of the TPs and, for each set of TPs, the values of the associated EDPs and PGAs.

3. NEW BENCHMARK STRUCTURES IN AN EXISTING CLASS

3.1 Necessity of new benchmark structures

The XAI algorithm estimates the EDPs and the PGAs of a real structure based on similarity criteria between the TPs of the real structure and the TPs of benchmark ones included in the current dataset (current knowledge). The estimate of the capacity PGAs of a real structure provided by the XAI model is more accurate if the real structure is well represented by the benchmark structures in the current dataset. Hence, higher accuracy is obtained if the class of structures contains benchmark structures with TPs similar to those of the real structure. Conversely, estimate of the capacity PGAs of a real structure whose TPs are different compared to those of benchmark structures in the

Co-funded by the European Union

Funded by the European Union. Views and opinions expressed are however those of the author(s) only and do not necessarily reflect those of the European Union. Neither the European Union nor the granting authority can be held responsible for them.

current dataset may be inaccurate. In this case the current dataset has to be improved by adding new benchmarks with TPs similar to those of the real structure under analysis. As a particular case, the real structure can be used as one of the new benchmarks. Figure 1 schematically shows a class of structures containing a certain number of benchmark structures, each represented by a red point. In this figure, a real structure is represented by a yellow square. In Figure 1a, the real structure is well represented by the current dataset, since several benchmark structures are close to it. Conversely, the real structure shown in Figure 1b is not well represented by the current dataset, since its distance with respect to the benchmark structures is high. In the first case, the XAI model provide a better estimation of the capacity PGAs of the real structure than in the second case.

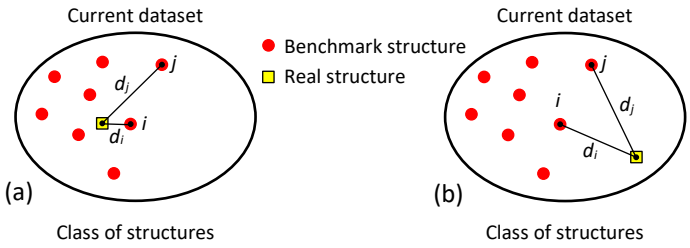

Figure 1. Distances between a real structure and benchmark structures. (a) Real structure is well represented by benchmark structures. (b) Real structure is not well represented by benchmark structures.

The definition of a metric in the space of the TPs, representing the distance between structures, is used to determine whether or not new benchmarks should be added to the dataset. In this project, the distance between a real structure and the generic j^{th} benchmark structure is defined based on the TPs as

$$d_j = \sqrt{\|\bar{\mathbf{p}} - \bar{\mathbf{q}}\|} = \sqrt{\sum_{i=1}^{n} \left(\bar{q}_i - \bar{p}_i^j\right)^2} \qquad (1)$$

where n is the number of TPs representing each benchmark and real structure of the class, $\bar{\mathbf{p}}^j = \left[\bar{p}_1^j, \bar{p}_2^j, \ldots, \bar{p}_n^j\right]$ is the array collecting the normalized TPs of the j^{th} benchmark structure and $\bar{\mathbf{q}} = \left[\bar{q}_1, \bar{q}_2, \ldots, \bar{q}_n\right]$ is the array collecting the normalized TPs of the real structures. Normalized TPs are defined such that each normalized TP of benchmarks is within the range [0;1], as

$$\bar{p}_i^j = \frac{p_i^j}{\max_{j=1,..,m}\left\{p_i^j\right\}} \qquad \text{for benchmark structures} \qquad (2)$$

Co-funded by the European Union

Funded by the European Union. Views and opinions expressed are however those of the author(s) only and do not necessarily reflect those of the European Union. Neither the European Union nor the granting authority can be held responsible for them.

$$\overline{q}_i = \frac{q_i}{\max_{j=1,..,m}\left\{p_i^j\right\}} \qquad \text{for real structures} \qquad (3)$$

where m is the number of benchmarks in the current dataset, $\mathbf{p}^j = \left[p_1^j, p_2^j, ..., p_n^j\right]$ and $\mathbf{q} = \left[q_1, q_2, ..., q_n\right]$ are the arrays collecting the TP of the j^{th} benchmark and real structures, respectively. The level at which a real strucutre is represented by the current dataset is based on the average distance of the real strucutre from benchmarks:

$$D = \frac{1}{m}\sum_{j=1}^{m} d_j \qquad (4)$$

and by the distances of the benchmark structures closer to the real one.

However, when parameter D is above a thresold value, the system can still determine the capacity PGAs even though results could be unsatisfactory. In this case the system will provide an alert suggesting to improve the current dataset.

Figure 2a shows a real structure which is not well represented by benchmark structures of the current dataset.

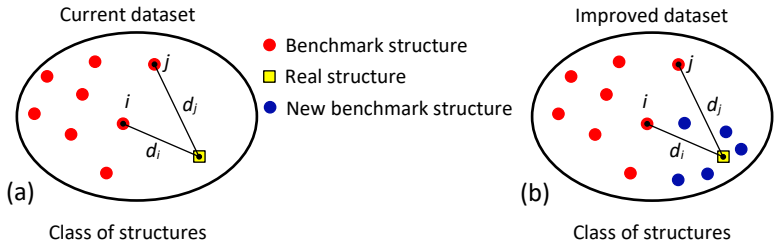

Figure 2. Distances between a real structure and benchmark structures. (a) Real structure is not well represented by benchmark structures in current dataset. (b) Improve of the dataset by adding new benchmarks.

In order to improve the accuracy of the estimation of its EDPs and PGAs, new benchmarks were added to the dataset. These are represented by the blue points in the improved dataset shown in Figure 2b. The TPs of new benchmarks were chosen similar to those of the real structure. The number of new benchmarks needed depends on the distance D, the distances d_j and the level of similarity of the TPs of new benchmarks with the TPs of the real structure. New benchmarks are continuously stored in the dataset and the improved dataset constitutes the current dataset for future seismic assessments. Thus, the system will continuously improve its accuracy in estimate EDPs and PGAs. Figure 3 schematically shows the procedure described.

Co-funded by the European Union

Funded by the European Union. Views and opinions expressed are however those of the author(s) only and do not necessarily reflect those of the European Union. Neither the European Union nor the granting authority can be held responsible for them.

3.2 Computation of EDPs and capacity PGAs

When a new benchmark structure is introduced in a current dataset, its EDPs and PGAs have to be computed via structural analysis and introduced in the dataset. The procedure for computing EDPs and PGAs depends on the type of structures. The procedures used for structures of reinforced concrete and masonry buildings and for earth retaining walls are summarized hereinafter.

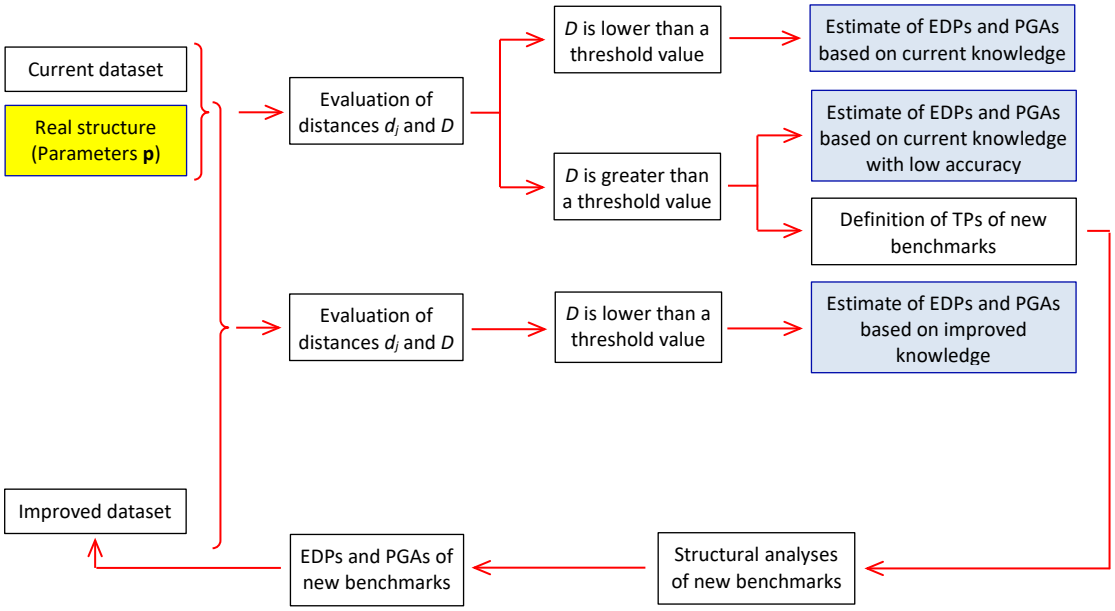

Figure 3. Necessity to improve the dataset of benchmark structures in a class.

3.2.1 Building structures

Structural analisys

For building with reinforced concrete and masonry structures, nonlinear pushover analysis according to the N2 method ([1], [2]) was used. In pushover analyses, the displacement d_c of a control point (typically the center of mass of the upper floor, named top displacement) is monotonically increased and the total lateral force, named base shear, associated with any displacement is computed (Figure 4). The total lateral force is applied according to a distribution proportional to a displacement shape $\boldsymbol{\phi}$

$$F_i = \alpha m_i \varphi_i \tag{5}$$

where α is a factor, F_i is the force applied to the i^{th} mass m_i, whose displacement in the displacement shape $\boldsymbol{\phi}$ is φ_i (i=1,2,…N, where N is the number of degrees of freedom of the system). The result of the pushover analysis is the relation between the top displacement d_c and the base shear V_b (Figure 4), named capacity curve (d_c-V_b). The peak base shear is denoted with V_{bu} and the corresponding

Co-funded by the European Union

Funded by the European Union. Views and opinions expressed are however those of the author(s) only and do not necessarily reflect those of the European Union. Neither the European Union nor the granting authority can be held responsible for them.

top displacement is denoted with d_m. A typical capacity curve is shown in Figure 5. At any step of the pushover analysis (i.e., for any value of d_c), the values of the EDPs are recorded and associated with the corresponding values of top displacement and base shear.

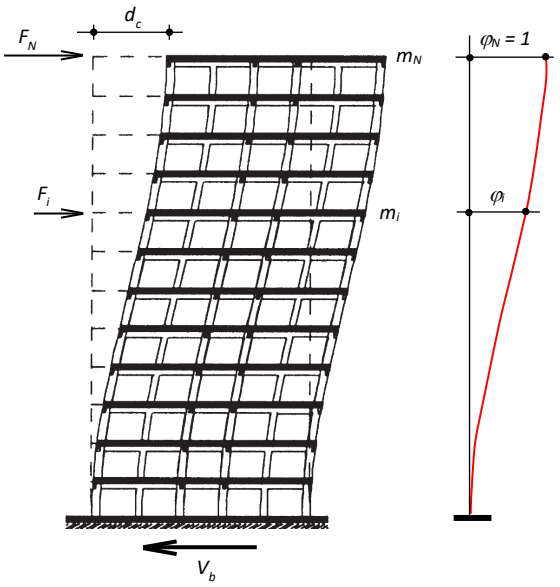

Figure 4. Pushover analysis (from [3]).

Since the levels of damage D1, D2, D3, and D4 (Deliverable 3.1) are associated with specific values of the EDPs, the top displacements (d_{c1}, d_{c2}, d_{c3}, and d_{c4}) and base shear corresponding to the levels of damage D1, D2, D3, and D4 can be identified in the capacity curve, as shown in Figure 5.

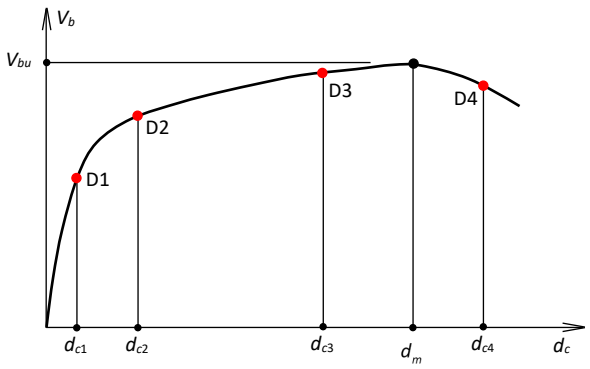

Figure 5. Capacity curve.

Levels of damage

For masonry structures, capacity is defined in terms of roof displacement d_c. In the MEDEA project, the indication given in [4] and [5] have been followed to determine displacements for each one of the four limit states defined in Deliverable 3.1. In particular, for D4, D3 and D2 reference has been

Co-funded by the European Union

Funded by the European Union. Views and opinions expressed are however those of the author(s) only and do not necessarily reflect those of the European Union. Neither the European Union nor the granting authority can be held responsible for them.

made to Annex C, Sec. C4.2 of [4], while for D1, being the limit state of operation not considered in [4], the provisions reported in [5] have been adopted. Assessment criteria are reported in the following:

- SLC (D4): displacement d_{c4} is taken equal to the roof displacement at which the total lateral resistance (base shear) has dropped below 80% of the peak resistance of the structure (base shear equal to $0.8V_{bu}$, Figure 5).
- SLV (D3): displacement d_{c3} is taken equal to 3/4 of the ultimate displacement capacity evaluated for SLC (D4).
- SLD (D2): for the damage limit state, displacement d_{c2} is defined as the yield point (yield force and yield displacement) of the idealized elasto-perfectly plastic force - displacement relationship of the equivalent Single-Degree-of-Freedom system (see next Section).
- SLO (D1): for the limit state of operation, the displacement d_{c1} is equal to 2/3 of d_{c2}.

Capacity of reinforced concrete structures, defined in terms of displacement, has been determined, for each one of the abovementioned four levels of damage, according to the indication given in [4] and [5]. In particular, for D4, D3 and D2 reference has been made to Annex A, Sec. A.3 of [4], while for D1, being the limit state of operation not considered in [4], the provisions reported in [5] have been adopted. It is worthwhile recalling that failure mechanisms of reinforced concrete structure are defined as *ductile* (i.e., those of beams, columns, and wall under flexure with and without axial force) and *brittle* (i.e., those related to shear mechanisms of beams, columns, walls, and joints). Assessment criteria are reported in the following:

- SLC (D4): displacement d_{c4} is defined as the roof displacement at which
  - the chord rotation (EDP) of one structural element attains its chord rotation capacity θ_{um} for *ductile mechanisms*;
  - the shear force (EDP) in one structural element attains its shear resistance V_R calculated in accordance with Sec. 5.2.4 of [6] or the strength in a beam-column joint is attained for *fragile mechanisms*.
- SLV (D3): displacement d_{c3} is defined as the roof displacement at which
  - the chord rotation (EDP) of one structural element attains 3/4 of its chord rotation capacity θ_{um} for *ductile mechanisms*;

Co-funded by the European Union

Funded by the European Union. Views and opinions expressed are however those of the author(s) only and do not necessarily reflect those of the European Union. Neither the European Union nor the granting authority can be held responsible for them.

- for *fragile mechanisms* the verification against the exceedance of this limit state is not required, unless it is the only one to be checked. If this is the case, provisions relevant to SLC (D4) applies.

- SLD (D2): displacement d_{c2} is defined as the roof displacement at which
  - the chord rotation (EDP) of one structural element attains its chord rotation at yielding θ_y for *ductile mechanisms*;
  - for *fragile mechanisms* the verification against the exceedance of this limit state is not required, unless it is the only one to be checked. If this is the case, provisions relevant to SLC (D4) applies.
- SLO (D1): for the limit state of operation, the displacement is defined by the attainment of a chord rotation equal to 2/3 of the one considered for SLD (D2).

Computation of the capacity PGAs

Top displacements d_{c1}, d_{c2}, d_{c3}, and d_{c4} are associated with the values of PGA producing their attainment using the procedure described hereinafter ([3], [7]).

From the capacity curve $d_c - V_b$ of the structure, the capacity curve $d_c^* - V_b^*$ of an equivalent single degree of freedom (SDOF) system having mass m^* is obtained by dividing the top displacement and the shear base by transformation factor Γ [2] (Figure 6):

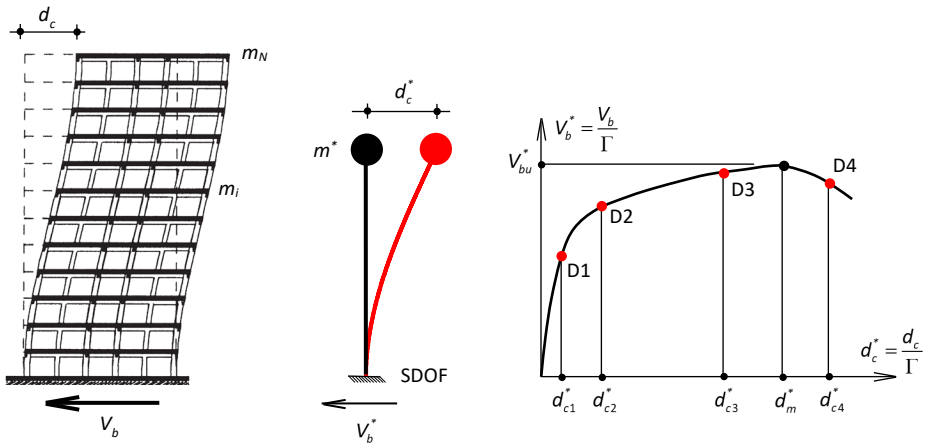

Figure 6. Equivalent SDOF.

$$m^* = \boldsymbol{\phi}^T \mathbf{M} \bullet \mathbf{1} \tag{6}$$

$$d_c^* = \frac{d_c}{\Gamma} \tag{7}$$

Co-funded by the European Union

Funded by the European Union. Views and opinions expressed are however those of the author(s) only and do not necessarily reflect those of the European Union. Neither the European Union nor the granting authority can be held responsible for them.

$$V_b^* = \frac{V_b}{\Gamma} \tag{8}$$

$$\Gamma = \frac{\boldsymbol{\phi}^T \mathbf{M} \boldsymbol{\tau}}{\boldsymbol{\phi}^T \mathbf{M} \boldsymbol{\phi}} \tag{9}$$

where **M** is the mass matrix, $\boldsymbol{\phi}$ is the array of displacements representing the displacements shape, normalized such that its maximum value is equal to 1.

The capacity curve $d_c^* - V_b^*$ of the SDOF system is then converted to an equivalent bilinear (elastoplastic) capacity curve $d_c^* - F^*$ (Figure 7).

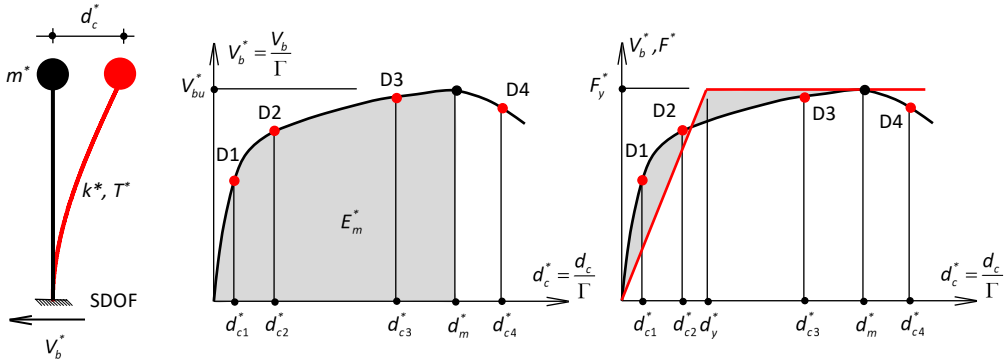

Figure 7. Equivalent bilinear SDOF.

The bilinear capacity curve is characterized by a yield displacement d_y^* and a plateau force F_y^*. F_y^* is defined as

$$F_y^* = V_{bu}^* = \frac{V_{bu}}{\Gamma} \tag{10}$$

whereas d_y^* is determined by enforcing that the areas under the actual and idealized capacity curves up to d_m^* are equal:

$$d_y^* = 2\left(d_m^* - \frac{E_m^*}{F_y^*}\right) \tag{11}$$

where E_m^* is the deformation energy up to d_m^* (Figure 7). The period T^* of the idealized equivalent bilinear SDOF system is

$$T^* = 2\pi\sqrt{\frac{m^* d_y^*}{F_y^*}} \tag{12}$$

Funded by the European Union. Views and opinions expressed are however those of the author(s) only and do not necessarily reflect those of the European Union. Neither the European Union nor the granting authority can be held responsible for them.

Displacement d_{ci} associated with the level of damage D*i* (*i*=1, 2, 3, 4) of the capacity curve corresponds to displacement

$$d_{ci}^{*}=\frac{d_{ci}}{\Gamma} \qquad \text{(i=1, 2, 3, 4)} \tag{13}$$

in the equivalente SDOF and bilinear SDOF. The PGA of the spectrum producing a maximum displacement equal to d_{ci}^{*} is the PGA producing the level of damage D*i*, i.e., the capacity PGA_{Di}. The procedure for obtaining the capacity PGAs was based on the pseudo-accleration elastic response spectrum $S_a(T)$ defined by Eurocode 8 [7], where *T* is the natural period of the elastic SDOF system and S_a is the maximum pseudo-acceleration of the mass of the SDOF system. The displacement elastic spectrum $S_d(T)$ is obtained from $S_a(T)$ as

$$S_d(T)=\frac{T^2}{4\pi^2}S_a(T) \tag{14}$$

In these spectra, T_C denotes the end of the constant branch of $S_a(T)$.

If $T^{*}\geq T_c$ (Figure 8), the displacement of the of the elasto-plastic SDOF is equal to the displacement of an elastic SDOF having the same stiffness [8]. Thus, in this case, among several spectra (each one corresponding to a PGA), the spectrum producing a maximum displacement equal to d_{ci}^{*} is determined as the one passing through the point with coordinate d_{ci}^{*} on the straigth line representing the period T^{*} in the acceleration-displacement plane (*Acceleration-Displacement Response Spectra,* ADSR, Fiigure 8b). The PGA of this spectrum is PGA_{Di} (Figure 8c).

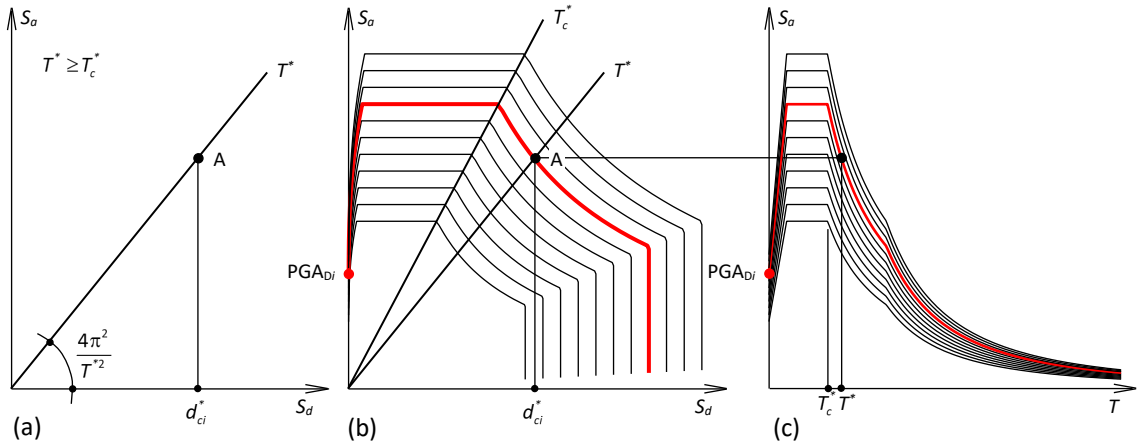

Figure 8. Determination of the capacity PGA_{Di} for $T^{*}\geq T_c$. (a) point corresponding to d_{ci}^{*} in the acceleration-

Funded by the European Union. Views and opinions expressed are however those of the author(s) only and do not necessarily reflect those of the European Union. Neither the European Union nor the granting authority can be held responsible for them.

displacement plane. (b) Acceleration-Displacement Response Spectra and PGA associated with d_{ci}^*. (c) Pseudo-acceleration spectra $S_a(T)$ and PGA associated with d_{ci}^*.

If $T^* < T_c$ (Figure 9), the displacement of the of the elasto-plastic SDOF is greater than the displacement of an elastic SDOF having the same stiffness [9].

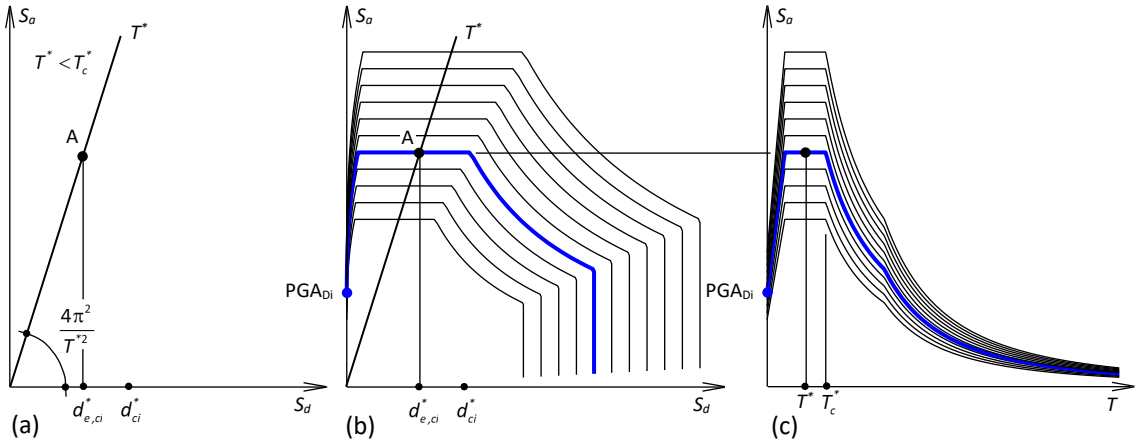

Figure 9. Determination of the capacity PGA_{Di} for $T^* < T_c$. (a) point corresponding to $d_{e,ci}^*$ in the acceleration-displacement plane. (b) Acceleration-Displacement Response Spectra and PGA associated with d_{ci}^*. (c) Pseudo-acceleration spectra $S_a(T)$ and PGA associated with d_{ci}^*.

The displacement d_{max}^* of the elasto-plastic SDOF can be related to the displacement $d_{e,max}^*$ of an elastic SDOF having the same stiffness as

$$d_{max}^* = \frac{d_{e,max}^*}{q}\left[1+(q-1)\frac{T_c}{T^*}\right] \tag{15}$$

where

$$q = \frac{S_a(T^*)m^*}{F_y^*} \tag{16}$$

Therefore, in this case, among several spectra (each one corresponding to a PGA), the spectrum producing a maximum displacement equal to d_{ci}^* for the elasto-plastic SDOF is determined as the one passing through the point with coordinate

$$d_{e,ci}^* = d_{ci}^* \frac{q}{1+(q-1)\frac{T_c}{T^*}} \tag{17}$$

on the straigth line representing the period *T** in the acceleration-displacement plane (*Acceleration-Displacement Response Spectra,* ADSR, Figure 9b). The PGA of this spectrum is PGA_{Di} (Figure 9c).

Co-funded by the European Union

Funded by the European Union. Views and opinions expressed are however those of the author(s) only and do not necessarily reflect those of the European Union. Neither the European Union nor the granting authority can be held responsible for them.

3.2.2 Earth retaining flexible walls

For earth retaining flexible walls, only the PGA producing the collapse of the wall, named PGA_C, was considered. Thus, when adding a new benchmark retaining wall to the class, its PGA_C has to be computed and introduced in the dataset.

Within the project, the collapse PGA of a retaining flexible wall was determined using finite element (FE) formulations of the limit analysis ([10]-[13]). The use of the of limit analysis theorems in a FE formulation allows to effectively determine the collapse PGA as a function of the TP describing the geometry of the wall and anchors and the soil properties. The collapse mechanism, i.e., the field of displacements. can also be associated with the collapse PGA.

In the Finite Element (FE) formulations of the limit analysis, the seismic action is represented by a system of horizontal accelerations whose intensity is the product of a multiplier k_h by the gravitational acceleration g (Figure 10). Multiplier k_h is increased until a state of incipient collapse is attained: in these conditions the soil-structure system fails because the equilibrium is no longer possible.

The value of k_h associated with the collapse of the system is referred to as the collapse multiplier and denoted with k_c. The upper– and lower–bound solutions of FE limit analyses identify the horizontal critical accelerations $g \cdot k_c$, and if sufficiently close to each-other, allow defining accurately the sought solution to the plastic collapse problem, also providing the plastic mechanism, i.e., the displacement field when collapse occurs. The collapse PGA is evaluated as

$$PGA_c = g \cdot k_c \tag{18}$$

Different collapse mechanisms were considered, as described in Deliverable 3.1.

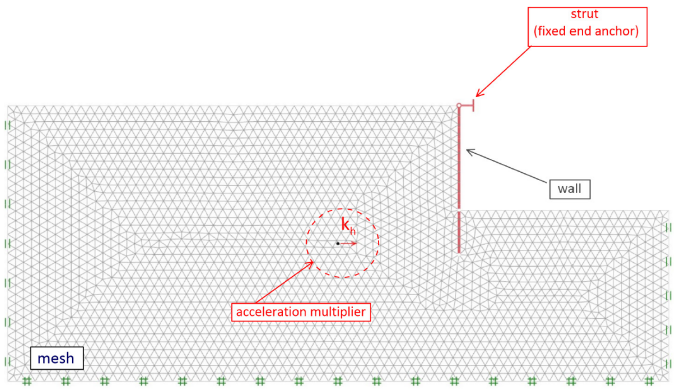

Figure 10. Finite element mesh of an earth retaining flexible wall and horizontal accelerations.

Co-funded by the European Union

Funded by the European Union. Views and opinions expressed are however those of the author(s) only and do not necessarily reflect those of the European Union. Neither the European Union nor the granting authority can be held responsible for them.

5. CONCLUSION

This deliverable provides criteria to define the new classes of structures and the new benchmark structures in an existing class. Each class includes structures that can be described by the same set of technical parameters (TPs). A new class of structure must be defined when it is necessary to evaluate via explainable Artificial Intelligence (XAI) the seismic capacity of a structure that can't be represented by the technical parameters (TPs) of the classes previously defined. The set of benchmark structures of a class has to be improved by adding new benchmark structures when it is necessary to evaluate via XAI the seismic capacity of a real structure with TPs different from those of current benchmark structures. The addition of new classes and new benchmarks continuously enlarges the knowledge base improving the accuracy of the XAI model to estimate the seismic capacity of real structures.

REFERENCES

[1] Fajar P, Krawinkler H. (editors). (1992). Nonlinear seismic analyses and design of reinforced concrete buildings. Elsevier Applied Science, London.
[2] Fajfar P. (2000). A nonlinear analysis method for performance based seismic design. Earthq Spectra 16(3):573–592.
[3] Mwafy AM, Elnashai AS. (2000). Static pushover versus dynamic collapse analysis of RC buildings. Engineering Structures 23:407-424.
[4] CEN EN 1998-3 Design of Structures for Earthquake Resistance - Part 3: Assessment and Retrofitting of Buildings. Brussels, Belgium, 2005.
[5] Ministero delle Infrastrutture e dei Trasporti Norme Tecniche per le Costruzioni. Rome, Italy, 2018 (*in Italian*).
[6] CEN EN 1998-1 Action on Structures. Brussels, Belgium, 2004.
[7] CEN EN 1998-1 Design of Structures for Earthquake Resistance - Part 1: General Rules, Seismic Actions and Rules for Buildings. Brussels, Belgium, 2005.
[8] Fajar P. (1999). Capacity spectrum method based on inelastic demand spectra. Earthquake Engineering and Structural Dynamics 28(9):979-993.
[9] Chopra AK, Goel RK. (1999). Capacity-demand-diagram methods for estimating seismic deformation of inelastic structures: SDF systems. Report PEER-1999/02. Pacific Earthquake Engineering Research Center, University of California, Berkeley, CA.
[10] Sloan S. (1988). Lower bound limit analysis using finite elements and linear programming, Int. J. Num. Anal. Meth. Geomech. 12:61–77.
[11] Sloan S. (1989). Upper bound limit analysis using finite elements and linear programming, Int. J. Num. Anal. Meth. Geomech. 13:263–282.
[12] Lyamin AV, Sloan S. (2002). Lower bound limit analysis using non-linear programming, Int. J. Num. Meth. Engng. 55:573–611.
[13] Lyamin AV, Sloan S. (2002). Upper bound limit analysis using linear finite elements and non-linear programming, Int. J. Num. Anal. Meth. Geomech. 26:181–216.

Co-funded by the European Union

Funded by the European Union. Views and opinions expressed are however those of the author(s) only and do not necessarily reflect those of the European Union. Neither the European Union nor the granting authority can be held responsible for them.